THESIS



#### ABSTRACT

## A THEORETICAL ANALYSIS OF AIR VELOCITY DISTRIBUTION INSIDE A VENTILATED ROOM WITH A LONG SLOT INLET

#### by Felleke Zawdu

The purpose of the research study is to derive a theoretical equation that will describe the air velocity distribution inside a mechanically ventilated room--given the quantity of air discharging into the room through a long narrow slot.

A theoretical analysis of a free jet discharged into open space and exhausted out through a circular sink was undertaken and an equation describing the mean air velocity magnitudes at given points inside the room was derived with the following general assumptions:

- 1. Flow is 3-dimensional
- 2. Flow is steady
- 3. Flow is incompressible

Then, an experimental study was conducted where readings of actual velocity magnitudes were taken inside a 9' x 8' x 2' framed box using a hot wire anemometer. The results of the theoretical and the experimental studies showing mean velocities versus distance were plotted. All the theoretical and experimental plots clearly exhibit

symmetries of velocity distributions about the center of the box. The theoretical as well as the experimental curves show higher velocity distributions at distances near the outlets and lower velocity magnitudes for points near the center of the box in both the x-y and x-z planes. Both the theoretical and the experimental curves also indicate higher velocity magnitudes at y = 0 and a gradual decline in velocity for points along |y| > 0 in the y-z plane. A general conclusion was reached where the shapes of the theoretical curves do follow the patterns of the experimental plots except where the physical boundaries of the box exaggerated the experimental velocity magnitudes of the air streams moving adjacent to these boundary layers.

Comparison of absolute velocity magnitudes was not made because the low air flow rate employed in the study induced correspondingly low air velocity distribution in In addition, experimental errors as well as the the box. inherent limitations of the theoretical derivations become significant in the velocity range less than 15 fpm--which is considered as stagnant air. Therefore, an unrealistic percent deviation between the theoretical and experimental valves results. A future research study employing air velocity of not less than 35 fpm--which is considered as satisfactory condition within the occupied zone--is sug-Approved: Melo L Esmay
Malor Professor gested.

# A THEORETICAL ANALYSIS OF AIR VELOCITY DISTRIBUTION INSIDE A VENTILATED ROOM WITH A LONG SLOT INLET

Ву

Felleke Zawdu

#### A THESIS

Submitted to

Michigan State University
in partial fulfillment of the requirements
for the degree of

MASTER OF SCIENCE

Department of Agricultural Engineering

#### ACKNOWLEDGMENTS

The author wishes to express his sincere appreciation to Professor M. L. Esmay of the Department of Agricultural Engineering, under whose general guidance this study was conducted.

The author also wishes to thank Dr. D. R. Heldman for the help rendered in instrumentation.

Appreciation is also extended to S. A. Weller for giving his assistance in writing programs for the computer.

#### TABLE OF CONTENTS

																		Page
ACKNO	WLE	EDGI	MEN	TS	•	•	•	•	•	•	•	•	•	•	•	•	•	11
LIST	OF	FI	GUR	ES	•	•	•	•	•	•	•	•	•	•	•	•	•	iv
INTRO	DUC	TIC	NC				•	•		•	•	•	•	•	•	•	•	1
OBJEC	TIV	Æ.	•	•		•	•	•		•	•	•	•			•	•	4
LITEF	RATU	JRE	RE	VIE	EW	•	•			•		•	•	•	•	•	•	5
	А.		Vе	nti	llat	io	n (	remen Condi Air	tic	ns	•	•		•	•	•	•	5 <b>7</b>
THEOF	-			•			•	•		•			•	•		•	•	13
	A. B.	Ki Po	ine ote	mat nti	cics Lal	s o Fl	f I	Fluid and	s Vel	· loci	itv	Pot	teni	tia		•	•	13
	C.	Sc	Fu our	nct	ior ar	n nd a	Sir				•	•	•	•	•		•	15 17 19
EXPER	RIME	ENTA	ΑL	STU	JDY	•	•	•			•		•			•	•	21
	A. B. C. D.	Ca Pr	ali coc	bra edu	ıre	on •	•	•		•	•	•	•	•	•	•	•	21 21 21 22
RESUL	TS.		•		•	•	•	•	•		•	•	•		•	•	•	28
	A. B.				ica nent		•	•			•	•	•			•	•	28 28
DISCU	ISSI	ON	OF	RE	ESUI	LTS	•	•		•	•	•	•			•	•	35
CONCL	usi	ONS	5			•	•	•			•		•	•		•	•	38
SUGGE	STE	ED I	TUT	URE	E RE	ESE.	ARO	CH.			•	•	•	•	•	•	•	40
REFER	RENC	ES.	•	•		•	•	•					•		•	•	•	41
4 10 10 10 10	( T T T																	1: 1:

#### LIST OF FIGURES

Figure		Page
1.	An Elementary Parallelepiped Fluid	13
2.	A Velocity Vector in Plane Polar Co-ordinate Axis	16
3.	A 3-Dimension Source of Radii of Spheres	17
4.	A Source-Sink Pair	19
5.	Box Elevation	25
6.	Box Side Views	25
7.	Venturi Tube	25
8.	Hot Wire Anemometer Filament Calibration Chart	26
9.	Pictorial View of Apparatus Set-Up and Instrumentation	27
10.	Hot-wire Anemometer Probe, Stand, and Probe Moving Mechanism	27
11.	Theoretical Velocity Magnitude versus Distance, x-y plane	29
12.	Theoretical Velocity Magnitude versus Distance, x-y plane	30
13.	Theoretical Velocity Magnitude versus Distance, y-z plane	31
14.	Experimental Velocity Magnitude versus Distance, x-y plane	32
15.	Experimental Velocity Magnitude versus Distance, x-z plane	33
16.	Experimental Velocity Magnitude versus Distance, y-z plane	34

#### INTRODUCTION

To obtain satisfactory results in ventilating, airconditioning and warm air heating systems correct air
distribution is highly essential. Even though a system
delivers to a room the required quantity of conditioned air,
unsatisfactory conditions will prevail if the air is poorly
distributed.

The purpose of air distribution in ventilating, airconditioning and warm air heating is to create in the occupied zone of the conditioned room the desired combination
of temperature, humidity, and air motion. To maintain comfort conditions within this zone, standard limits have been
established as acceptable effective temperatures comprising
of air temperature, motion, humidity and the physiological
effect on the surface of the human body. Any variation
from accepted standards of one of these elements or lack of
uniformity of conditions within the occupied space or excessive fluctuation of conditions in the same part of the
space may result in discomfort to the occupants. Such discomfort may be due to excessive room air temperature variations (horizontally, vertically, or both), excessive air
motion (draft), failure to deliver or distribute the air

according to the load requirements at the different locations, or too rapid fluctuation of room temperature or air motion.

To create optimum environmental conditions ventilation air exchanges are highly critical in confined housing of livestock and poultry. Air temperature and relative humidity affect the amount of heat and water dissipation and hence the productivity of livestock and poultry. In any confined animal housing operation either natural or mechanical ventilation, although the latter system is preferred, is designed to remove the moisture given off by the animals as rapidly as it is produced. The ideal ventilation rate would be generally geared to maintain the desired moisture balance at lower outside temperatures and the optimum heat balance at higher outside temperatures.

Variations in building construction, system designs, and operating requirements make practical room air distribution problems quite complex. To analyze the performance of a jet discharged from any air supply outlet, the engineer needs answers to these questions:

- What is the throw of the air jet?
- What is its angle of divergence or spread and its velocity profile?
- 3. How can velocity at any given point within the jet be determined?

This thesis is directed towards question no. 3 and hence determining the velocity distribution of an air jet discharged into a room.

#### OBJECTIVE

Many confined livestock and poultry housing operations use mechanical ventilation systems where exhaust fans perform the necessary air exchange discharging into the houses through long narrow crack inlets or slots. The objective of this research study is to formulate a theoretical equation that describes the velocity distribution of an air jet discharged into a room through a long slot and exhausted through a circular hole; and to compare the theoretical results with values obtained by taking measurements of actual velocity magnitudes at the specified points inside the room.

#### LITERATURE REVIEW

Literature is reviewed in regard to the following two general aspects of ventilation:

- A. Standard requirements for optimum ventilation conditions.
- B. Theory of room air distribution.

### A. Standard Requirements for Optimum Ventilation Conditions

Barre and Sammet (2) state that air circulation may be required to remove moisture from a livestock shelter, to cool a room or the products stored in it, to dry or humidify the atmosphere or a product, or to maintain a standard of air purity. Barre and Sammet (2) present the Moisture-Balance equation as:

$$M = \frac{W_{e}}{\mu_{2}W_{s_{2}} - \mu_{1}W_{s_{1}}}$$
 (1)

where, M = air flow per hour, lb.

 $W_e$  = moisture to be exchanged per hour, lb.

 $\mu_2$  and  $\mu_1$  = degree of saturation in outgoing and incoming air, respectively (for practical purposes  $\mu$  usually may be assumed equal to the relative humidity)

W and W = water in saturated air-vapor mixtures at temperature of outgoing and incoming air, respectively, lb./lb. dry air.

and the Heat-Balance equation as:

$$Q_L + Q_s + M_a (0.24)(t_o - t_i) + A U_{AV}(t_o - t_i) = 0$$
 (2)

where,  $Q_{T}$  = latent heat exchanged, Btu/hr.

 $Q_s = sensible-heat input, Btu/hr.$ 

 $M_a = air flow per hour, lb.$ 

A = total surface area exposed to temperature difference,  $ft^2$ 

to and t = outside and inside air temperatures,
 respectively

U<sub>AV</sub> = average overall heat-transmission coefficient (a weighted average in which the U value of each type of wall is included in proportion to its area).

ASHAE Guide (1) points out that velocities less than 15 fpm generally cause a feeling of air stagnation, whereas velocities higher than 65 fpm may result in a sensation of draft. The Guide further reports that air velocities of 25 to 35 fpm in the occupied zone are considered satisfactory, but air motion of 20 to 50 fpm will usually be acceptable.

In housing swine, Hazen and Mangold (10) mention that moisture and odor produced by the swine are to be removed by ventilation; and in particular where there is large differential between the inside and outside temperatures, necessary amounts of air can create draftiness even though the velocity is low. Hazen and Mangold (10) further state that since a heat-balance of a swine-production unit reveals there is inadequate sensible heat production by the animal to maintain wide temperature differentials between outside

and inside, the required supplemental heat could be used effectively to prevent drafts by preheating the ventilating air prior to the time it comes into contact with the animal.

Cargill, Stewart, and Johnson (4) report that the ideal design environment-controlled summer shelter for dairy cows could be based on a limiting discomfort index of 75.

The discomfort index is defined by the relationship:

D1 = 
$$0.55 T_{db} + 0.2 T_{dp} + 17.5$$
 (3)

where, D1 = discomfort index

Tdb = dry-bulb temperature

 $T_{dp} = dew-point temperature.$ 

Esmay (6) states that an actual ventilation air exchange of 3 cfm per square foot of floor area should be provided for poultry laying houses in the northern zones of the United States during the warmer seasons of the year. Esmay (6) further reports that a practical, economical and effective ventilation system is the exhaust type where the exhaust fans are to be located and air is discharged into the house from the attic through a long narrow crack inlets of 1- to 1½-inches wide.

#### B. Theory of Room Air Distribution

The theory of room air distribution is not complete, but a considerable fund of knowledge supported by experimental guidance is available for the solution of many air distribution problems. Tuve (21) points out that both

engineers and scientists have paid much attention to the free jet problem. A free jet is one discharged into a relatively large room or other free atmospheric space. Limitations are imposed that no surfaces or objects are near enough to the stream to interfere with the formation of the natural flow-pattern and that the primary stream is straight-flowing, free from pulsations and helical flow. Tuve (21) established four major zones along the direction of a free jet. These zones are roughly defined in terms of the maximum or center-core velocity that exists at the cross-section being considered.

- Zone 1: A short zone of 2 to 6 diameters from the outlet face. Core-velocity is very nearly equal to the original outlet velocity throughout the length.
- Zone 2: A transition zone that usually extends 8 to 10 diameters. The maximum velocity may vary inversely as the square root of the distance from the outlet.
- Zone 3: An extensive zone of 25 to 100 diameters long, depending on the shape and area of the outlet and initial velocity. Maximum velocity varies inversely as the distance from the outlet.
- Zone 4: A terminal zone in which the residual velocity decays into a large scale turbulence. The maximum velocity subsides to the range below 50 fpm usually regarded as still air.

These four zones indicated above do not fully describe the performance of a free jet. Tuve (21) states that the laws of continuity, conservation of momentum, conservation of energy, and dimensional analysis have been applied to the analysis of free jets. Vorticity transfer theory has

also been developed. Tuve (21) further states that all the mathematical formulations defining jet performance call for experimental constants and in many cases these are not as yet well established. Therefore, by treating the air as an incompressible fluid and assuming that viscous flow is not encountered, Tuve (21) shows that the maximum center-core velocity in Zone 3 can be determined with good engineering accuracy for round outlets from the equation:

$$V_{x} = \frac{K' Q}{x \sqrt{A_{o}}} \qquad (4) \qquad \text{where}$$

- Q = volume of air discharged from outlet per unit time.
- A<sub>o</sub> = effective area of stream at discharge.
  - X = distance from outlet
     face.
- K' = proportionality constant.

Tuve (21) further indicates that theoretically, for an infinite slot the center-core velocity varies as the square root of the distance.

$$V_C(X)^{\frac{1}{2}} = C \tag{5}$$

In regard to boundary layer problems Tuve (21) mentions that Nottage demonstrated clearly that when the axis of a long jet is too close to the wall, floor or ceiling, and parallel with it, the spread of the jet in that direction is reduced and a greater throw of the air stream occurs with the wall in place than that of the jet discharging into free open space from the same outlet.

Koestel and Austin (12) in analyzing the maximum velocity in a jet stream issuing from two parallel nozzles using the principle of conservation of momentum derived an equation to determine the maximum center-line velocity at a given distance from the outlet face for a single jet as:

$$\rho \ V_{c}^{2} = \frac{a}{2} D_{o}^{2} \rho \ V_{o}^{2} \tag{6}$$

$$\rho V^2 = \frac{a}{2} D_0^2 \rho V_0^2 e^{-2ar^2}$$
 (7)

where,  $a = \frac{c_2}{x^2}$ , a shape factor

 $c_2 = 2 k^2$ 

k = constant, length in diameters
 of the constant velocity core

x = distance, ft

 $V_{o}$  = outlet velocity, ft/sec.

 $D_{o}$  = diameter of nozzel, ft.

V<sub>c</sub> = jet velocity along stream lines through the nozzel, ft./sec.

 $\rho$  = air density, slug/cubic foot

V = jet velocity at radius r, at distance x, ft./sec.

r = radius, ft.

e = the base for the Napierian system of logarithms e = 2.718

Koestel (11) applying the principle of conservation of momentum states that the maximum center-line jet velocity can be found by the equation:

$$V_{c}/V_{o} = \frac{\sqrt{k(H_{o}/R_{o}) \cos \theta[k(H_{o}/R_{o}) \cos \theta + 1]}}{\sqrt{R(R_{o}-R_{o})}}$$
(8)

where,  $V_c$  = maximum velocity in air jet, fpm

 $V_{O}$  = maximum outlet velocity, fpm

R = distance from geometric center of outlet to where maximum jet velocity is V<sub>c</sub>, ft.

 $R_{o}$  = radius of outlet, ft.

H = width of slot opening in outlet, ft.

k = length of the constant velocity core
in terms of the width, H

θ = horizontal deflection of axis stream, degrees

Elrod (5) in presenting a theoretical analysis of the performance of a jet states that Reichardt hypothesized that "momentum diffuses with distance from a source in the same manner that heat-energy diffuses with the square root of time." Then Elrod (5) further states that by analogy with the well-known equation of heat conduction the following equation may be written:

$$\frac{\partial \rho W^2}{\partial (z^2)} = \frac{c^2}{4} \left[ \frac{\partial^2 \rho W^2}{\partial x^2} + \frac{\partial^2 \rho W^2}{\partial y^2} \right] \tag{9}$$

Elrod (5) then presents a general equation for the computation of experimental results as:

$$\frac{W}{W_{O}} = \sqrt{\frac{\left\{\frac{\operatorname{erf}(\frac{x+a}{cz}) - \operatorname{erf}(\frac{x-a}{cz})}{2}\right\}\left\{\frac{\operatorname{erf}(\frac{y+b}{cz}) - \operatorname{erf}(\frac{y-b}{cz})}{2}\right\}}$$
(10)

where, W = time-mean velocity in z-direction

 $W_{\odot}$  = mean peak velocity of the source

a = half-width of infinite slot along
 x-axis

b = half-width of infinite slot along
y-axis

c = empirical constant in Reichardt's
 turbulence. Equation Approximate
 Value: 0.08

x = Cartesian coordinate in plane of jet source

y = Cartesian coordinate in plane of jet source

z = Cartesian coordinate in plane of jet source.

Elrod (5) concludes that with varying degrees of success, but with an accuracy sufficient for almost all engineering purposes, the free turbulence equation of Reichardt correlates the performance of free jets; and that value of 0.0805 for the constant c in equation (9) provides satisfactory agreement with the experiment.

#### THEORETICAL ANALYSIS

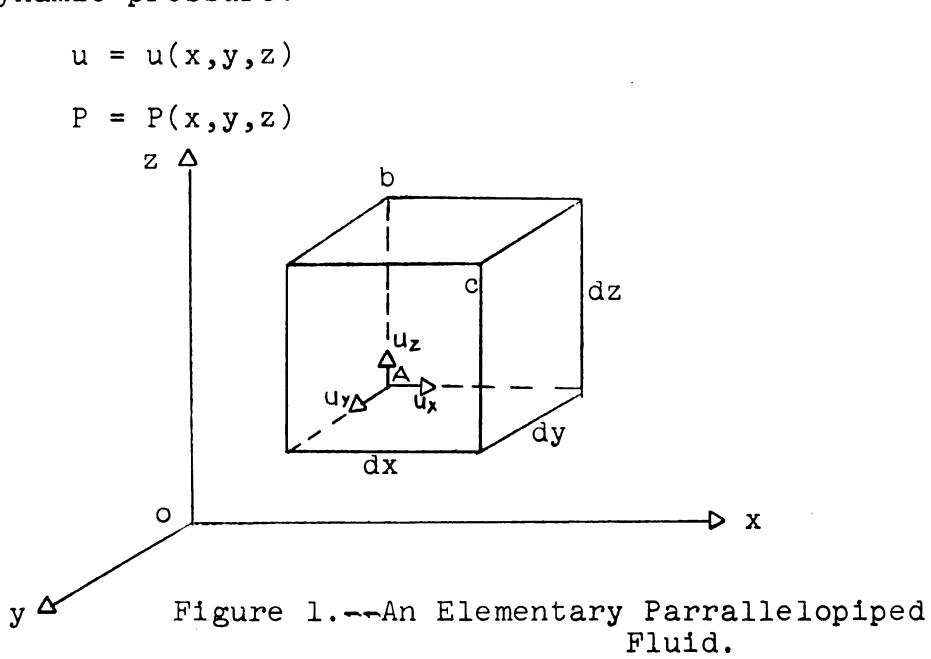
#### A. Kinematics of Fluids

The kinematics of fluids is the branch of science dealing with the laws of motion of a fluid. The fluid is considered to be a continuum and its motion is treated as the continuous and constructive deformation of a continuous material medium. To describe mathematically the velocity distribution of the fluid motion certain assumptions will have to be made.

#### Assumptions:

- 1. Flow is steady
- 2. Flow is 3-dimensional

Therefore, if u is the velocity vector and P is the hydro-dynamic pressure:



In the co-ordinate axes above, the parallelepiped of volume dxdydz containing a point A, moving at velocity  $\mathbf{U}_{A}$ , simultaneously participates in three types of motion-translation, deformation and rotation (Cauchy-Helmholtz Theorem, Reference 16).

Therefore, if  $U_A$  is the velocity of point A in the moving fluid, then the velocity of any point c is the geometrical sum of three velocity vectors — the translation velocity  $U_A$ , the deformational velocity  $U_{\mathrm{def}}$ , and the rotational, or vortex, velocity  $U_{\mathrm{rot}}$  about an instantaneous axis through A.

$$\overline{U}_{c} = \overline{U}_{A} + \overline{U}_{def} + \overline{U}_{rot}$$
 (11)

Cauchy-Helmholtz Equation (Reference 16)

This equation may be written (Reference 16):

$$U_{x(c)} = U_{x} + \left[\frac{\partial U_{x}}{\partial x}dx + \theta_{y}dz + \theta_{z}dy\right] + (\Omega_{y}dz - \Omega_{z}dy)$$

$$U_{y(c)} = U_{y} + \left[\frac{\partial U_{y}}{\partial y}dy + \theta_{z}dx + \theta_{x}dz\right] + (\Omega_{z}dx - \Omega_{x}dz) \qquad (12)$$

$$U_{z(c)} = U_{z} + \left[\frac{\partial U_{z}}{\partial z}dz + \theta_{x}dy + \theta_{y}dx\right] + (\Omega_{x}dy - \Omega_{y}dx)$$

 $\rm U_{x}, \, \rm U_{y}, \, \rm U_{z}$  are the translation velocity components, the terms in brackets are the deformational velocity components, and the terms in parentheses are the rotational velocity components, where (Reference 16):

$$\theta_{X} = \frac{1}{2} \left( \frac{\partial U_{Z}}{\partial y} + \frac{\partial U_{Y}}{\partial z} \right) \qquad \qquad \Omega_{X} = \frac{1}{2} \left( \frac{\partial U_{Z}}{\partial y} - \frac{\partial U_{Y}}{\partial z} \right)$$

$$\theta_{Y} = \frac{1}{2} \left( \frac{\partial U_{X}}{\partial z} + \frac{\partial U_{Z}}{\partial x} \right) \qquad \qquad \Omega_{X} = \frac{1}{2} \left( \frac{\partial U_{X}}{\partial z} - \frac{\partial U_{Z}}{\partial x} \right) \qquad (13)$$

$$\theta_{Z} = \frac{1}{2} \left( \frac{\partial U_{Y}}{\partial x} + \frac{\partial U_{X}}{\partial y} \right) \qquad \qquad \Omega_{Z} = \frac{1}{2} \left( \frac{\partial U_{X}}{\partial x} - \frac{\partial U_{X}}{\partial y} \right)$$

## B. Potential Flow and Velocity Potential Function

For an incompressible fluid undergoing potential flow the vorticity vector and its components are all zero (Reference 16); that is:

$$\Omega_{X} = \frac{1}{2} \left( \frac{\partial U_{Z}}{\partial y} - \frac{\partial U_{Y}}{\partial z} \right) = 0$$

$$\Omega_{Y} = \frac{1}{2} \left( \frac{\partial U_{X}}{\partial z} - \frac{\partial U_{Z}}{\partial x} \right) = 0$$

$$\Omega_{Z} = \frac{1}{2} \left( \frac{\partial U_{Y}}{\partial x} - \frac{\partial U_{X}}{\partial y} \right) = 0$$
(14)

Or

$$\frac{\partial U_{Z}}{\partial y} = \frac{\partial U_{y}}{\partial z}$$

$$\frac{\partial U_{x}}{\partial z} = \frac{\partial U_{z}}{\partial x}$$

$$\frac{\partial U_{x}}{\partial z} = \frac{\partial U_{x}}{\partial z}$$
(15)

These equations indicate that the velocity components  $U_x$ ,  $U_y$ ,  $U_z$  at each point of an irrotational fluid flow may be written as partial derivatives of some function  $\phi(x,y,z)$ ,

(Reference 16), that is:

$$U_{X} = \frac{\partial \phi(x,y,z)}{\partial x}$$

$$U_{Y} = \frac{\partial \phi(x,y,z)}{\partial y}$$

$$U_{Z} = \frac{\partial \phi(x,y,z)}{\partial z}$$
(16)

In the xy plane the function  $\phi$  depends on two variables only, so that equation (16) becomes, (Reference 16):

$$U_{x} = \frac{\partial \phi(x,y)}{\partial x}$$

$$U_{y} = \frac{\partial \phi(x,y)}{\partial y}$$
(17)

In plane polar co-ordinates these equations have the form (Reference 16):

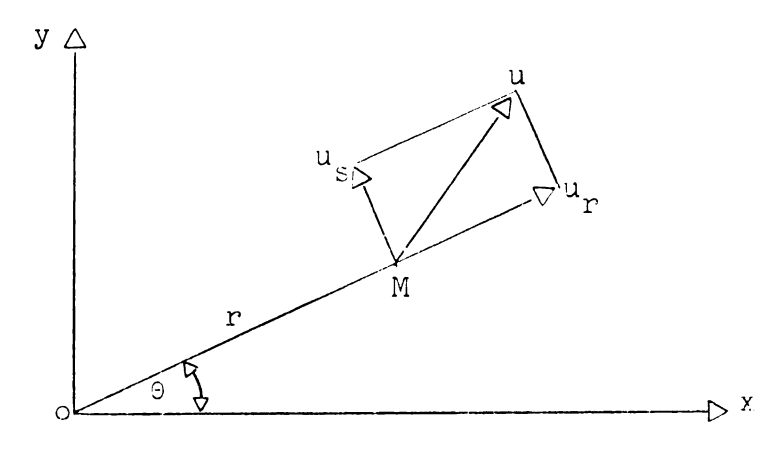


Figure 2.--A Velocity Vector in Plane Polar Co-ordinate Axis.

$$U_{\mathbf{r}} = \frac{\partial \phi}{\partial \mathbf{r}}$$

$$U_{\mathbf{s}} = \frac{\partial \phi}{\partial \mathbf{s}} = \frac{1}{\mathbf{r}} \frac{\partial \phi}{\partial \theta}$$
(18)

Where  $U_r$  and  $U_s$  are the radial and tangential components of the velocity vector U at point M (Figure 2).

#### C. Sources and Sinks

A source is a particular point in the space filled by the fluid, from which fluid enters the surrounding medium at some rate Q.

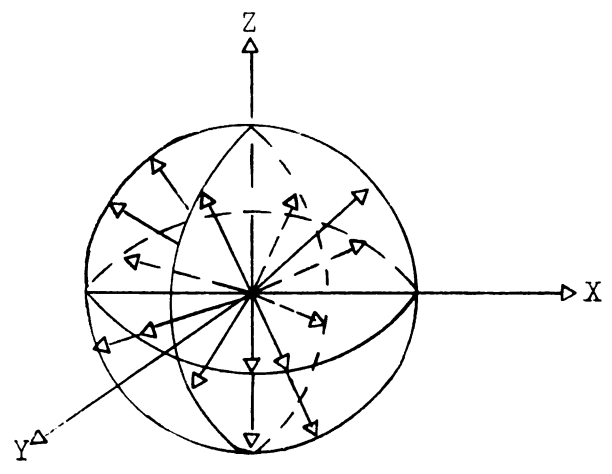


Figure 3.--A 3-Dimension Source of Radii of Spheres

The streamlines of the fluid are directed along the radii of the spheres drawn with the source as the center (Figure 3). A sink is a particular point at which fluid disappears at a rate Q. Consider a sphere of radius r measured from a source or sink, where source streamlines

have arbitrarily, a positive direction and sink streamlines have a negative direction. The flow velocity from a source or to a sink is then (Reference 16):

$$U = U_{r} = \pm \frac{Q}{\omega} = \pm \frac{Q}{4\pi r^{2}}$$
 (19)

In this case equations (18) reduce to (Reference 16):

$$U_{S} = 0; U_{r} = + \frac{d \varphi}{dr}$$
 (20)

Equations (19) and (20) give (Reference 16):

$$d\phi = \pm \frac{Q dr}{4\pi r^2} \tag{21}$$

The velocity components are (Reference 16):

$$U_{x} = \frac{\partial \phi}{\partial x} = \frac{\partial}{\partial x} (\mp \frac{Q}{4\pi r})$$

$$U_{y} = \frac{\partial \phi}{\partial y} = \frac{\partial}{\partial y} (\mp \frac{Q}{4\pi r})$$

$$U_{z} = \frac{\partial \phi}{\partial z} = \frac{\partial}{\partial z} (\mp \frac{Q}{4\pi r})$$
(23)

#### D. A Source--Sink Pair

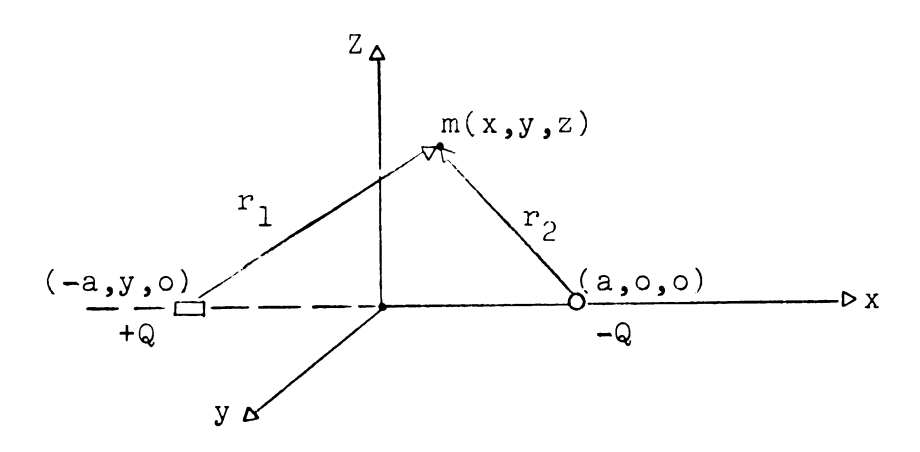


Figure 4

Consider a long slot source located at (-a,y,0) and a circular sink located at point (a,0,0) on an imaginary coordinated axes x,y,z as shown in Figure 4. The distance from an arbitrary point m(x,y,z) to the source  $r_1$  and the sink  $r_2$  are:

$$r_1 = \sqrt{(x+a)^2 + z^2}$$

$$r_2 = \sqrt{(x-a)^2 + y^2 + z^2}$$
(24)

The velocity potential function, equation (22) is in this case

$$\Phi(x,y,z) = \frac{Q}{4\pi} \{ [(x-a)^2 + y^2 + z^2]^{-\frac{1}{2}} - [(x+a)^2 + z^2]^{-\frac{1}{2}} \}$$
 (26)

Therefore the velocity components are:

$$U_{x} = \frac{\partial \phi}{\partial x} = \frac{Q}{4\pi} \left\{ \frac{(x+a)}{[(x+a)^{2}+z^{2}]^{3/2}} - \frac{(x-a)}{[(x-a)^{2}+y^{2}+z^{2}]^{3/2}} \right\}$$

$$U_{y} = \frac{\partial \phi}{\partial y} = -\frac{Qy}{4\pi[(x-a)^{2}+y^{2}+z^{2}]^{3/2}}$$

$$U_{z} = \frac{\partial \phi}{\partial z} = \frac{Qz}{4\pi} \left\{ \frac{1}{[(x+a)^{2}+z^{2}]^{3/2}} - \frac{1}{[(x-a)^{2}+y^{2}+z^{2}]^{3/2}} \right\}$$

$$V_{mean} = \sqrt{U_{x}^{2} + U_{y}^{2} + U_{z}^{2}}$$
(28)

#### EXPERIMENTAL STUDY

#### A. Apparatus Used

- 1. An exhaust fan
- 2. A venturi tube
- 3. A micro-manometer
- 4. A hot-wire anemometer set-up
- 5. A pitot tube
- 6. A 9' x 8' x 2' box built from plywood; one side covered with glass.

#### B. <u>Calibration</u>

The hot-wire anemometer was calibrated in a wind tunnel using a pitot tube and a micro-manometer. Readings for zero velocity or still air and for maximum velocity were taken and the necessary calibration curve of  $I^2$  vs.  $V^{\frac{1}{2}}$  was drawn as shown in Figure 8.

#### C. Procedure

The venturi tube was connected to the fan by a 4-inch diameter U-pipe and the set up was mounted to the 4-inch diameter outlet as shown in Figure 9. The micro-manometer was carefully installed to the venturi connections. After checking that all connections were air-tight, the fan was started and readings were taken from the micro-manometer

scale. These readings were averaged and the computed average was used to calculate the rate of air flow, Q, discharging into the box.

An imaginary x,y,z co-ordinate axes as shown in Figure 5 was drawn through the center of the box with the x-axis passing through the center of the exhaust outlet and the mid-point of the center line of the slot inlet. The probe of the hot-wire anemometer was placed inside the box and careful measurements of mean velocities were taken at the specified points with reference to the imaginary co-ordinate axes. At a given point three different measurements were taken by rotating the probe and hence the axis of the probe filament:

- The axis of the probe filament parallel to y-z plane.
- The axis of the probe filament parallel to x-y plane and facing towards the y-axis.
- 3. The axis of the probe filament parallel to x-y plane and facing towards the x-axis.

#### D. Calculations

#### 1. Flow rate, Q:

Assuming an expansion factor of 1, i.e., assuming that the air is incompressible (Reference 2):

$$Q = C M A_2 \sqrt{2g/\gamma} \sqrt{P_1 - P_2}$$
 (29)

$$= C M A_2 \sqrt{2gh}$$
 (30)

Where, 
$$M = \frac{1}{\sqrt{1 - (A_2/A_1)}} = \frac{1}{\sqrt{1 - (\frac{1}{4})^2}} = 1.033$$

C = 0.965 (Discharge Coefficient, from Beckwith and Buck)

h = 0.1 ft. of water (from micro-manometer)

 $= 0.1 \times 62.4 \times 13.5 = 84.25 \text{ ft. of air}$ 

$$A_2 = \pi (\frac{1}{12})^2 = 0.0218 \text{ ft.}^2$$

$$g = 32.2 \text{ ft./sec.}^2$$

$$\therefore$$
 Q = 0.965 x 1.033 x .0218  $\sqrt{2x32.2x84.24}$  x60 = 95.82 CFM

#### 2. Mean velocity

At a specified point inside the box three different measurements were taken as indicated above in Procedure.

Let A, B, and C be the velocity measurements obtained respectively at a given point inside the box with the axis of the filament aligned in the aforementioned directions using the established co-ordinated axes as a frame of reference. Since the hot-wire anemometer filament detects velocity magnitudes along two perpendicular planes, then:

$$\sqrt{V_{x}^{2} + V_{y}^{2}} = A$$

$$\sqrt{V_{y}^{2} + V_{z}^{2}} = B$$

$$\sqrt{V_{y}^{2} + V_{z}^{2}} = C$$
(31)

The measured values A, B, and C were programmed and fed into the computer and the magnitudes for the velocity components  $V_x$ ,  $V_y$ , and  $V_z$ ; and for V mean were obtained:

where, V mean = 
$$\sqrt{V_{x}^{2} + V_{y}^{2} + V_{z}^{2}}$$
 (32)

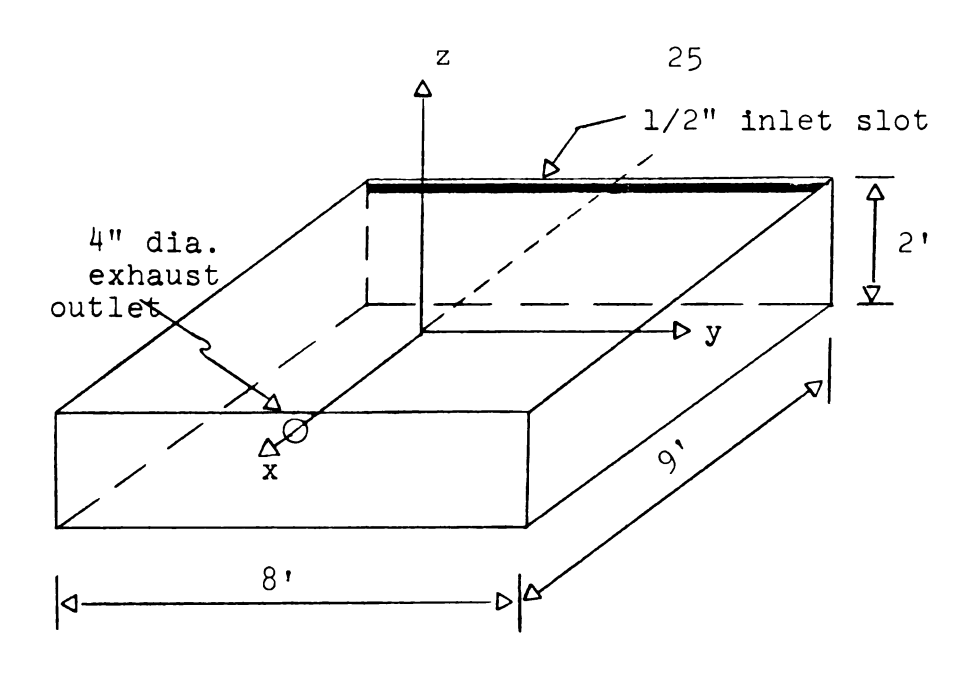


Figure 5.--Box Elevation

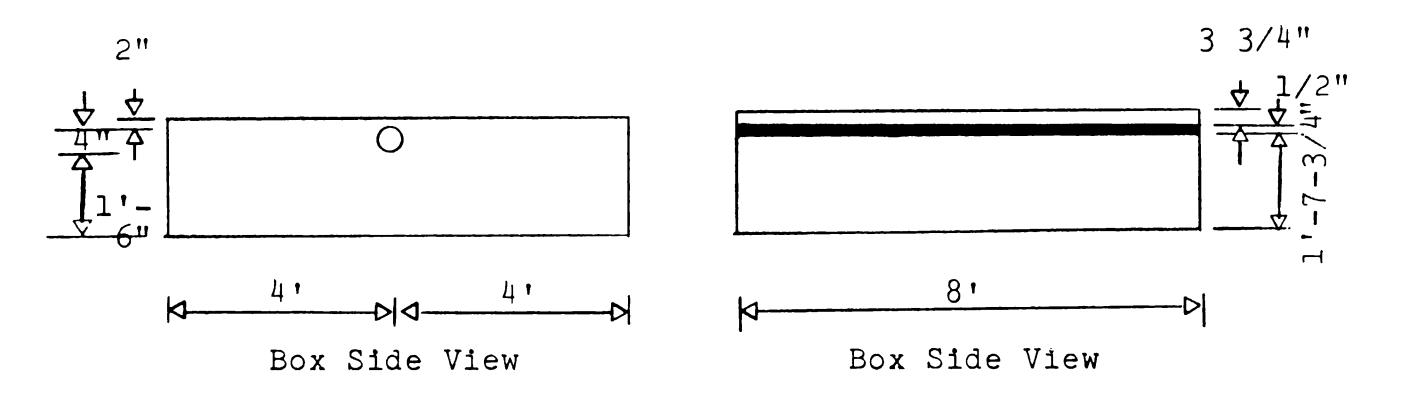


Figure 6.--Box Side Views

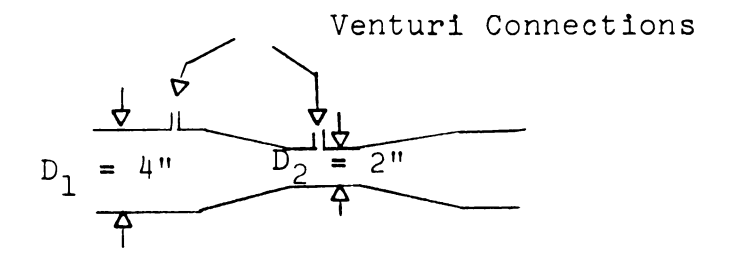
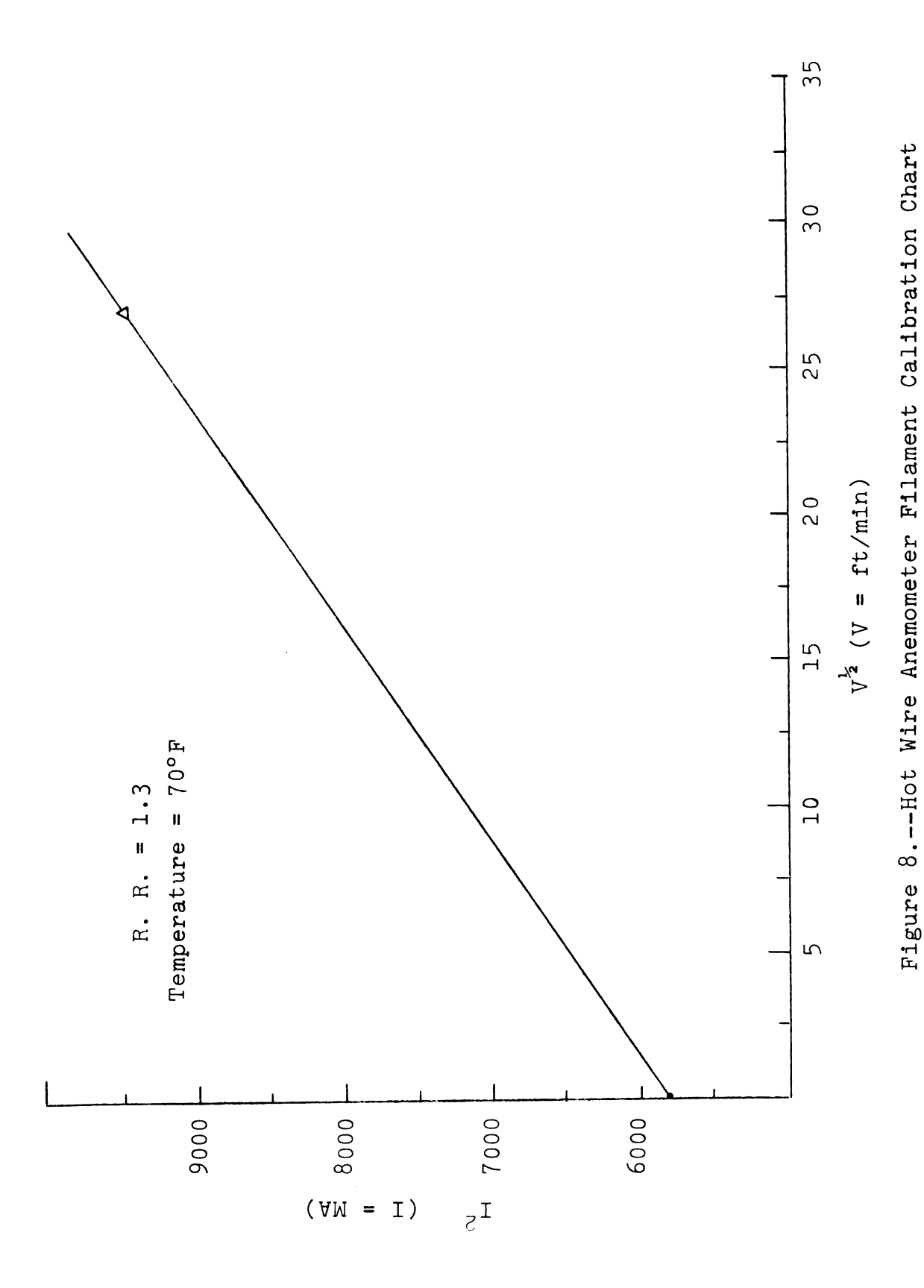


Figure 7.--Venturi Tube



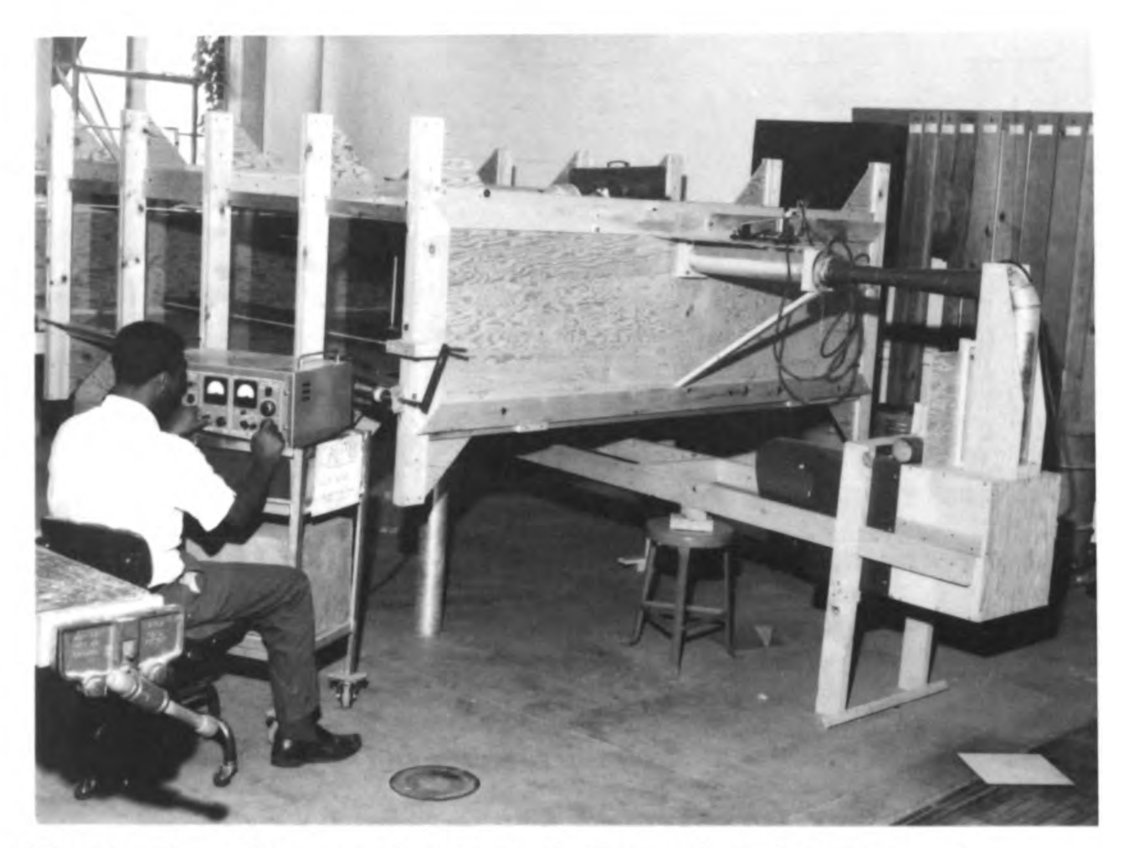


Figure 9.--Pictorial View of Apparatus Set-up and Instrumentation.

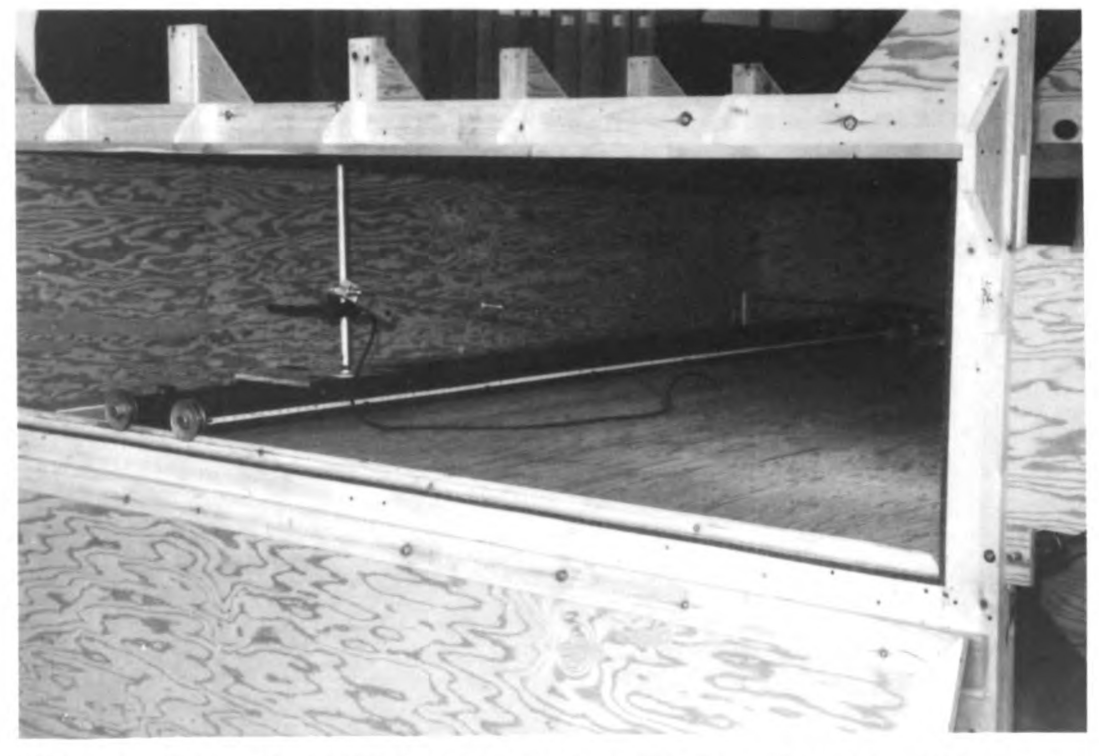


Figure 10.--Hot Wire Anemometer Probe, Stand, and Probe Moving Mechanism.

#### RESULTS

#### A. Theoretical

Q = 95.82 CFM (see page 23) was substituted into the theoretical velocity component equations and their magnitudes were calculated for given values of x,y,z, in reference to the established co-ordinate axes x,y,z within the box. Then, V mean =  $\sqrt{U_{\rm X}^2 + U_{\rm Y}^2 + U_{\rm Z}^2}$  was computed for these desired points. The results are shown graphically, Figures 11, 12, and 13, by plotting the mean velocities against distance.

#### B. Experimental

Measurements of velocity magnitudes at points corresponding to the theoretical case were taken and V mean  $= \sqrt{V_{\mathbf{x}}^2 + V_{\mathbf{y}}^2 + V_{\mathbf{z}}^2} \text{ (see page 23) was computed for each point.}$  The results are plotted on graph papers, Figures 14, 15, and 16, showing mean velocities versus distance.

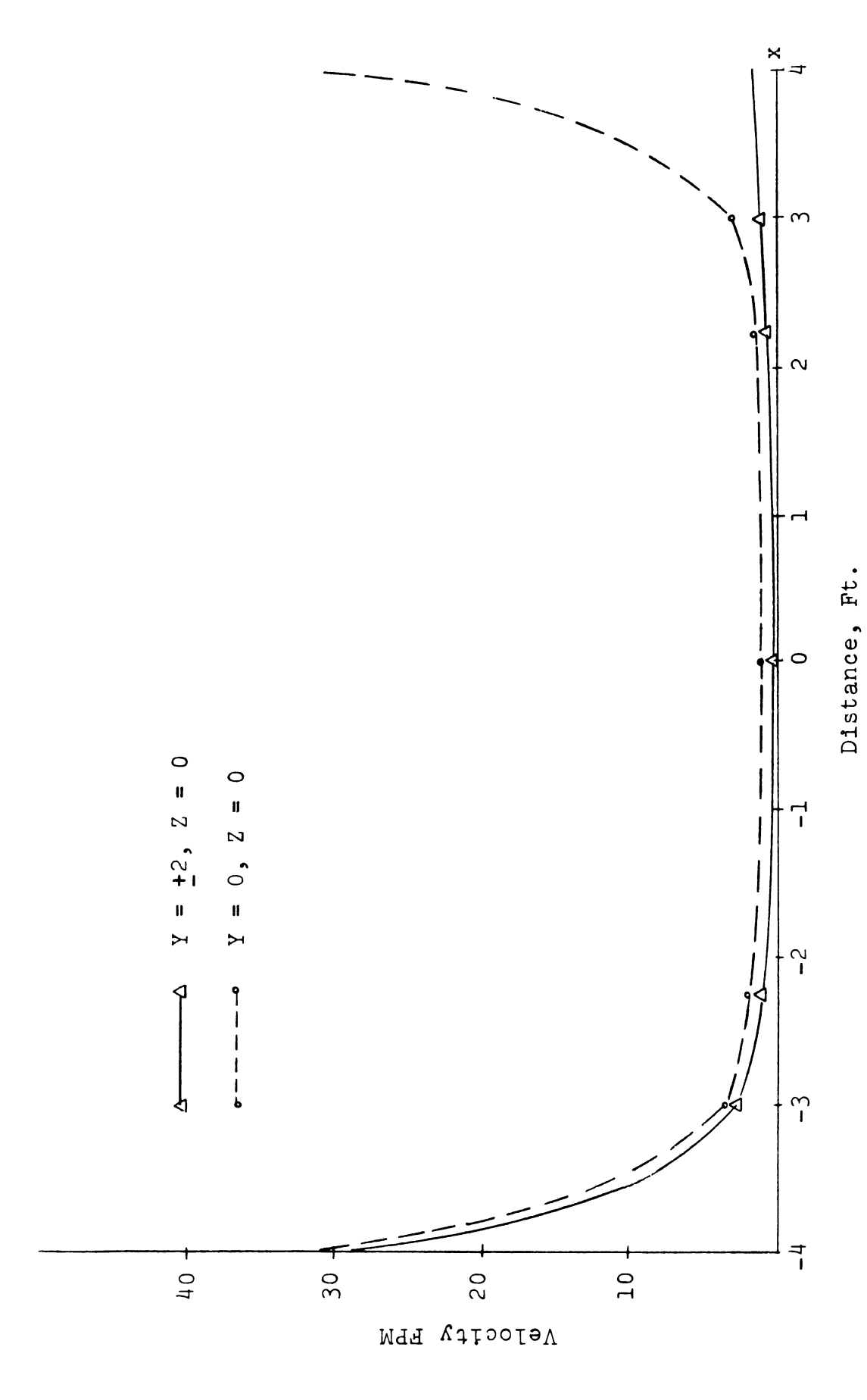


Figure 11. -- Theoretical Velocity Magnitude Versus Distance, x-y Plane

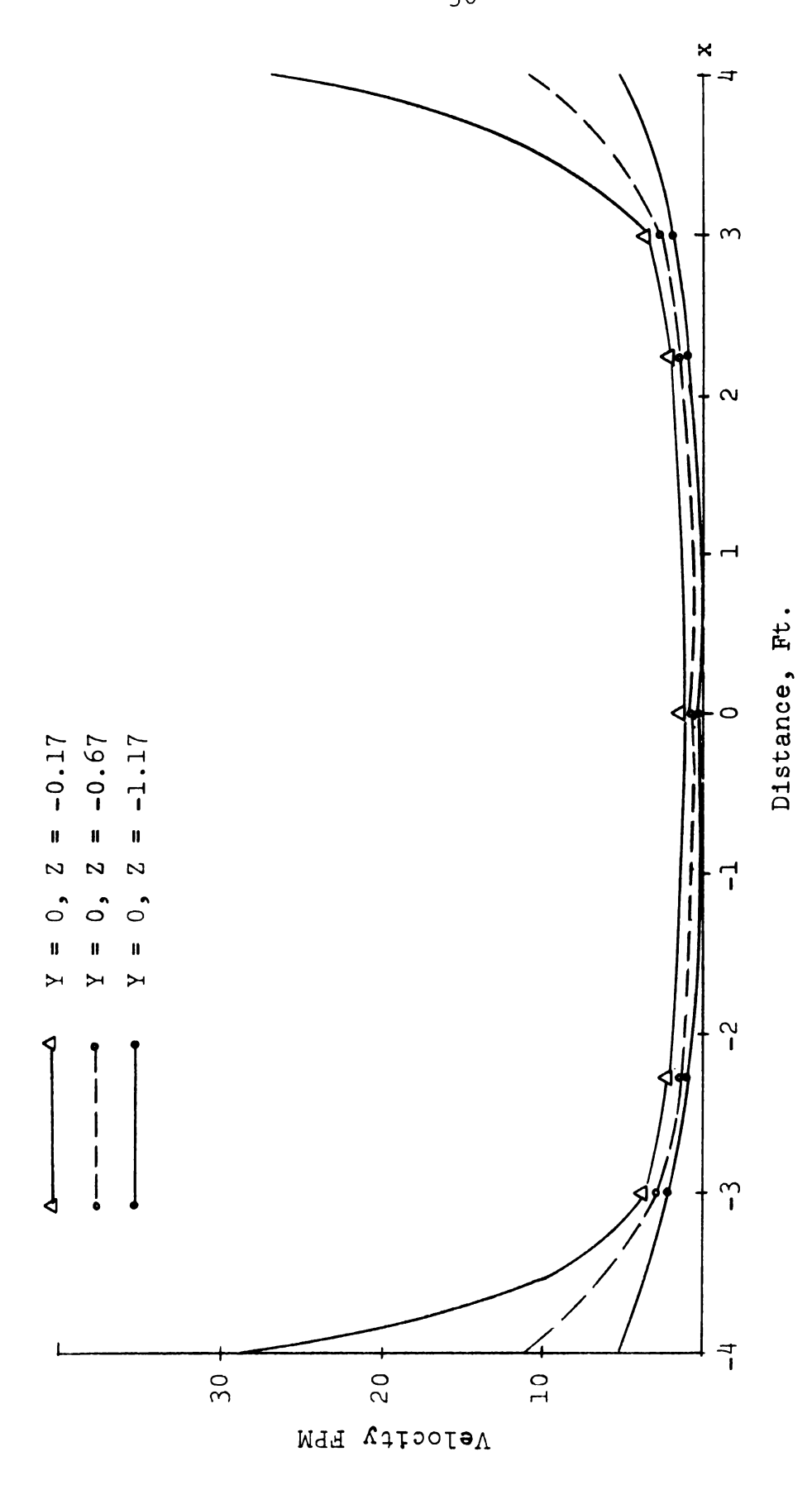


Figure 12. -- Theoretical Velocity Magnitude Versus Distance, x-z Plane

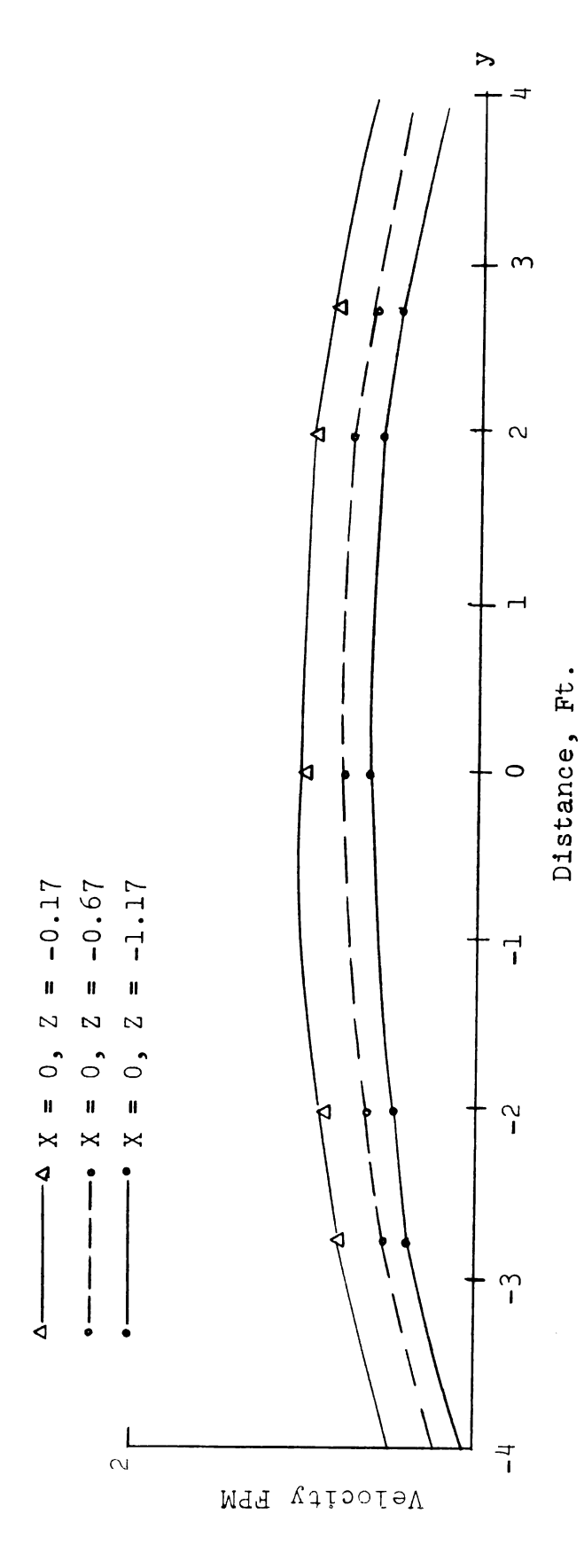


Figure 13.--Theoretical Velocity Magnitude Versus Distance, y-z Plane

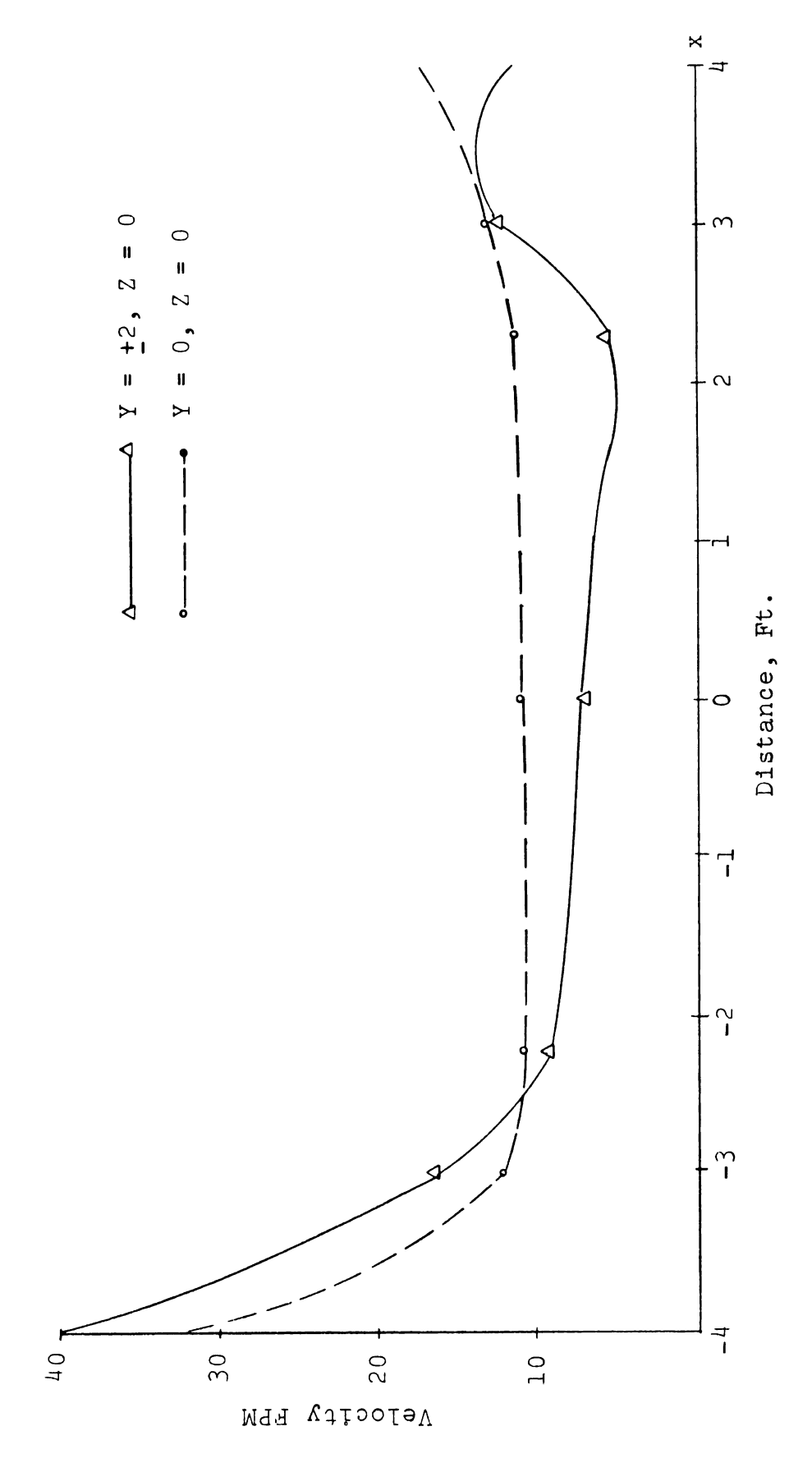


Figure 14.--Experimental Velocity Magnitude Versus Distance, x-y Plane

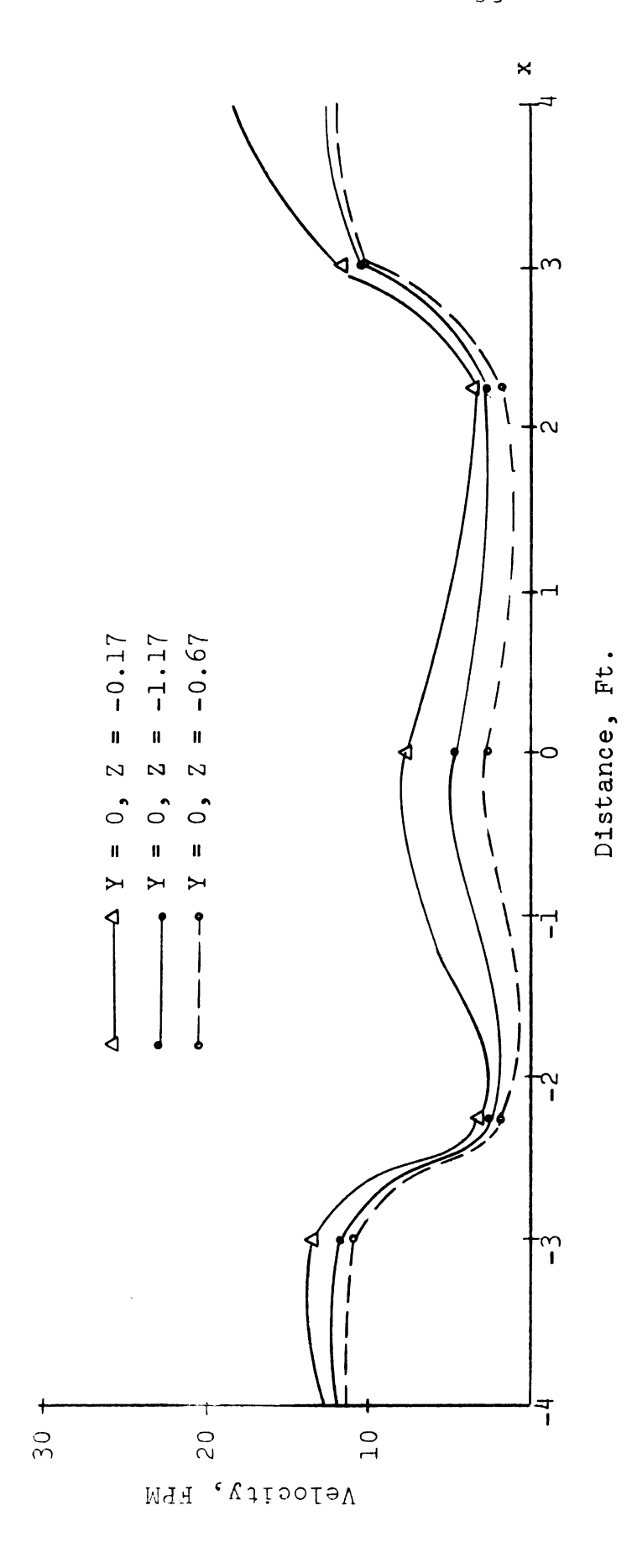


Figure 15.--Experimental Velocity Magnitude Versus Distance, x-z plane

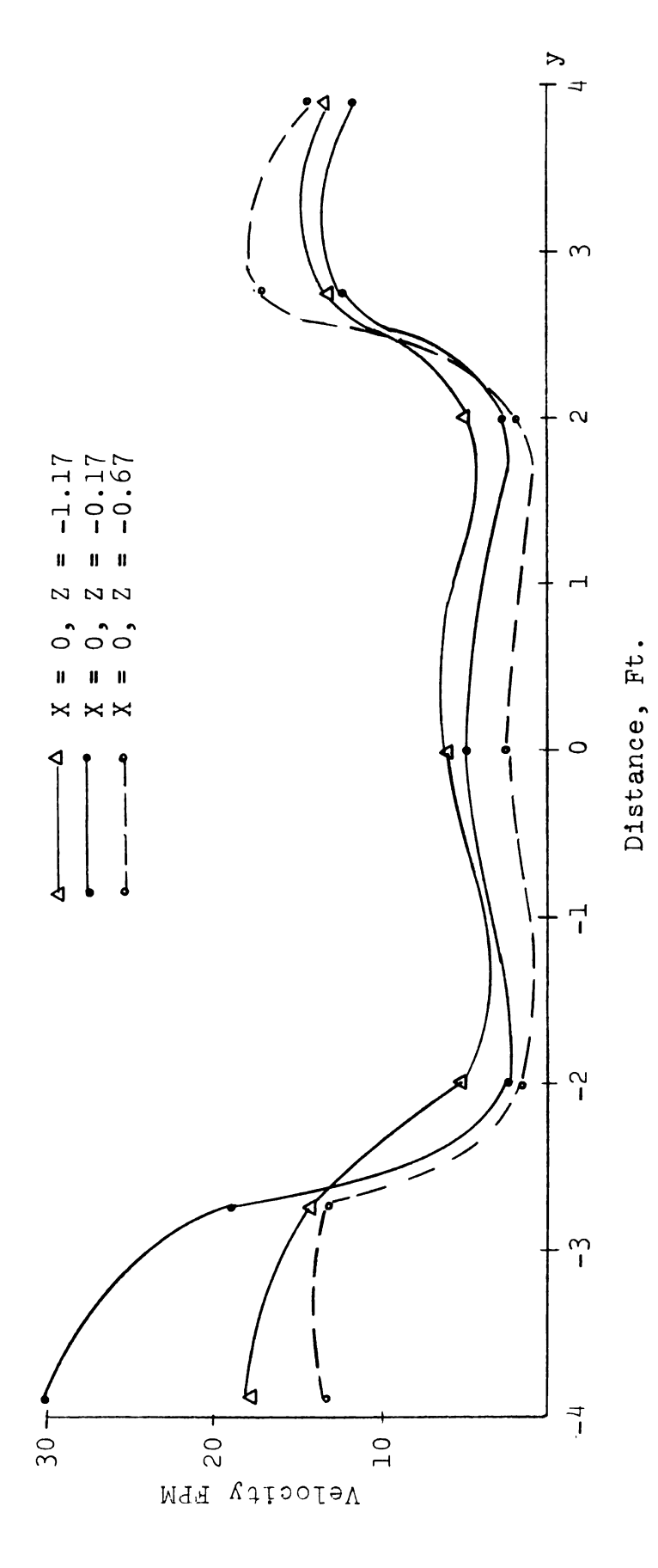


Figure 16. -- Experimental Velocity Magnitude Versus Distance, y-z Plane

### DISCUSSION OF RESULTS

Figures 11 and 14 show the velocity distribution for the theoretical and experimental investigations respectively in the x-y plane along the x-axis. The general shape of the plots of the theoretical case do correspond to that of the experimental curves.

Figures 12 and 15 indicate the velocity distribution in the x-z plane along the x-axis. The theoretical curves, Figure 12, predict smooth mean velocity distribution with low velocity magnitudes occurring around the center of the box at x = 0. Figure 12 also shows the Y = 0, Z = -0.67curve falling above the Y = 0, Z = -1.17 curve while the experimental curves, Figure 15, show the opposite. This is due to the bottom floor of the box which is a physical boundary and creates or promotes reflections and a greater throw to the bottom layer of the moving air, and hence causes an increase in the mean velocity magnitude of the bottom part of the moving air layer. In regard to boundary layers, Tuve (21), as mentioned in the literature review, points out that when the axis of a long jet is close to the wall or floor a greater throw of air stream results than a jet discharging into free open space which the theoretical curves, Figure 12, represent.

Figures 13 and 16 indicate the velocity distributions in the y-z plane along the y-axis. The shape of the plots of the theoretical case, Figure 13, correspond to that of the experimental curves, Figure 16, between the interval  $-2 \le y \le 2$ . However, between the intervals |2| > y the theoretical curves show a decline and the experimental curves show a rise in mean velocity magnitudes. This is again explained, as mentioned above, in terms of the sides of the box acting as physical boundaries and hence contributing to greater mean velocity magnitudes along the extreme right and left side layers of the moving air inside the box.

Discussions regarding the merits and acceptance of each plot and any comparison between corresponding theoretical and experimental curves has been geared to aspects concerning the shape of the curves rather than the absolute magnitudes each curve represents. Such an analysis or approach is taken because of the low flow rate, Q, employed in the study induced correspondingly low air velocity distribution in the box. In addition, the sources of error introduced in conducting the experimental study and the inherent limitations of the theoretical equations become significant at the low velocity range of less than 15 fpm. Hence, an unrealistic absolute average percent deviation between the experimental and theoretical investigations results. Here, average percent deviation is defined as:

$$\sum_{\text{Average \% of Deviation}} \frac{\sum_{\text{e}} |\frac{V_{\text{e}} - V_{\text{t}}}{V_{\text{e}}}| \times 100}{V_{\text{e}}}$$

where,  $V_{a}$  = experimental velocity readings

 $V_{+}$  = theoretical velocity prediction

N = total number of readings

Some of the sources of error and limitations of the equations are:

# 1. Sources of error

- a. Minor periodical fluctuations of the fan capacity resulting into unsteady flow rate conditions.
- b. Imperfect alignment of the hot-wire anemometer probe filament to face perpendicular to the direction of air flow.
- c. Human error in reading the true velocity measurements, caused mainly by turbulence.

# 2. Characteristics and limitations of the theoretical equations

- a. Flow is steady.
- b. Flow is incompressible.
- c. No physical boundary conditions, i.e., the air jet is discharged into free open space.

#### CONCLUSIONS

The following results based on the theoretical and experimental studies were obtained.

- Symmetries of velocity distribution about the center of the box do occur for all the theoretical and experimental plots.
- 2. The theoretical as well as the experimental curves show higher velocity distribution at distances near the outlets and lower velocity magnitudes near the center of the box in both x-y and x-z planes.
- 3. Both the theoretical and experimental plots indicate higher velocity magnitudes at y = 0 and a gradual decline in velocity for points along |y| > 0 in the y-z plane.
- 4. In the x-z plane the experimental curves show the y = 0, z = -0.67 curve falling below the y = 0, z = -1.17 curve, while the theoretical curves show the opposite.
- 5. In the y-z plane the shapes of the theoretical curves correspond to that of the experimental plots between the interval -2 < y < 2. However, between the intervals |2| > y the theoretical curves show a decline and the experimental curves show a rise in velocity magnitudes.

In general, the shapes of the theoretical curves do follow that of the patterns of the experimental plots with the aforementioned exceptions where certain boundary conditions of the box modify the predictions of the theoretical equation.

Since the sources of error involved in conducting the experimental study and the inherent limitations of the theoretical equations become significant at the low air velocity magnitudes of less than 15 fpm--which is considered as stagnant air--the average percent deviation will not be a realistic value.

# SUGGESTED FUTURE RESEARCH

- 1. A higher flow rate, Q, that will not yield a mean velocity magnitude of less than 35 fpm--which is considered as satisfactory air flow within the occupied zone-should be employed and the degree of acceptance of the average percent deviation could then be realistically analyzed.
- 2. A study of the effects of boundary layers on velocity distribution of adjacent air streams.

REFERENCES

#### REFERENCES

- 1. ASHAE: Heating Ventilating Air-conditioning Guide--Air distribution. ASHAE Guide, 1959, p. 267.
- 2. Barre, H. J., and L. L. Sammet. <u>Farm Structures</u>. New York: John Wiley and Sons, Inc., 1963.
- 3. Beckwith, T. G., and N. L. Buck. <u>Mechanical Measure-ments</u>. Massachusetts: Addison-Wesley Publishing Co., Inc., 1961.
- 4. Cargill, B. F., R. E. Stewart, and H. D. Johnson.
  Environmental Physiology and Shelter Engineering
  --Effect of humidity on total room heat and vapor
  dissipation of Holstein cows. University of
  Missouri Research Bulletin 794, 1962.
- 5. Elrod, H. G., Jr. "Computation charts and theory of rectangular and circular jets," ASHVE Research Report No. 1515. ASHVE Transactions, 60, (1954), p. 431.
- 6. Esmay, Merle L. "Design Analysis for Poultry-House Ventilation," Journal of Agricultural Engineering, Vol. 41, No. 9 (September, 1960), pp. 576-78.
- 7. Ginzburg, I. P. Applied Fluid Dynamics. Jerusalem: Israel Program for Scientific Translations, 1963.
- 8. Haerter, Alex A. "Flow distribution and pressure change along slotted or branched ducts," ASHRAE Research Report No. 1816. ASHRAE Transactions, 69, (1963), p. 124.
- 9. Hayes, F. C., and W. F. Stoeker. "Velocity patterns at return-air inlets and their effect on flow measurement," ASHRAE Research Report No. 1912.

  ASHRAE Transactions, 71 (1965), p. 37.
- 10. Hazen, T. E., and E. W. Mangold. "Functional and Basic Requirements of Swine Housing," <u>Journal of Agricultural Engineering</u>, 41, 9 (September, 1960), pp. 585-90.

- 11. Koestel, Alfred. "Jet velocities from radial flow outlets," ASHAE Research Report No. 1618.
  ASHAE Transactions, 63 (1957), p. 505.
- 12. Koestel, Alfred and J. B. Austin, Jr. "Air velocities in two parallel ventilating jets," ASHAE Research Report No. 1580. ASHAE Transactions, 62 (1956), p. 425.
- 13. Koestel, Alfred and G. L. Tuve. "The discharge of air from a long slot," ASHVE Research Report No. 1328. ASHVE Transactions, 54 (1948), p. 87.
- 14. Kratz, A. P., A. E. Hershey and R. B. Engdahl.
  "Development of instruments for the study of air
  distribution in rooms," ASHVE Research Report No.
  1165. ASHVE Transactions, 46 (1940), p. 351.
- 15. Madison, R. D., and W. R. Elliot. "Throw of air from slots and jets," ASHVE Journal, Section, Heating, Piping and Air Conditioning (November, 1946), p. 108.
- 16. Mkhitaryan, A. M. <u>Hydraulics and Fundamentals of Gas</u>

  <u>Dynamics</u>. Jerusalem: Israel Program for Scientific

  Translations, 1964.
- 17. Nelson, D. W., and D. J. Stewart. "Air distribution from side wall outlets," ASHVE Research Report No. 1076. ASHVE Transactions, 44 (1938), p. 77.
- 18. Nottage, H. B., J. G. Slaby and W. P. Gojsaza. "A V-wire direction probe," ASHVE Research Report No. 1441. ASHVE Transactions, 58 (1952), p. 79.
- 19. "Isothermal ventilation--jet fundamentals,"

  ASHVE Research Report No. 1443. ASHVE Transactions,
  58, (1952), p. 107.
- 20. Richardson, E. G. <u>Dynamics of Real Fluids</u>. London: Edward Arnold Publishers, LTd., 1961.
- 21. Tuve, G. L. "Air velocities in ventilating jets,"
  ASHVE Research Report No. 1476. ASHVE Transactions,
  59, (1953), p. 261.
- Tuve, G. L., D. K. Wright, Jr., and L. J. Seigel.
  "The use of air velocity meters," ASHVE Research
  Report No. 1140. ASHVE Transactions, 45 (1939),
  p. 645.

# APPENDIX

Table Showing Velocity Magnitudes at Specified Points Inside the Box

Plane	Point (x,y,z), ft.	Theoretical Vmean, fpm	Experimental Vmean, fpm
<b>x</b> - <b>y</b>	<b>-</b> 4.25, 2 , 0	122.0	126.5
	-4.0 , 2 , 0	30.5	39.8
	-3.5 , 2 , 0	7.7	10.3
	-3.0 , 2 , 0	3.5	16.2
	-2.5 , 2 , 0	2.0	19.6
	<b>-</b> 2.25, 2 , 0	1.6	9.1
	0, 2, 0	0.7	6.5
	2.25, 2, 0	1.0	3:3
	3.0 , 2 , 0	1.3	11.0
	3.5 , 2 , 0	1.6	11.6
	4.0 , 2 , 0	1.8	13.1
	<b>-4.25, 0 , 0</b>	122.0	148.7
	-4.0 , 0 , 0	30.5	32.7
	<b>-3.5</b> , 0 , 0	7.7	11.1
	-3.0 , 0 , 0	3.5	11.9
	<b>-2.5</b> , 0 , 0	2.0	22.8
	<b>-2.25,</b> 0,, 0	1.7	10.5
	0, 0, 0	0.8	11.3
	2.25, 0, 0	1.7	11.5
	3.0,0,0	3.5	13.0
	3.5 , 0 , 0	7.7	15.6
	4.0,0,0	30.6	16.5

Plane	Point (x,y,z), f		Theoretical Vmean, fpm	Experimental Vmean, fpm
<b>x</b> - <b>y</b>	-4.25, -2.0	), 0	122.0	148.7
	<b>-</b> 4.0 , <b>-</b> 2.0	), 0	30.6	46.6
	-3.5 , -2.0	), 0	7.7	19.1
	-3.0 , -2.0	), 0	3.5	21.6
	-2.5 , -2.0	), 0	2.0	31.0
	-2.25, -2.0	0, 0	1.7	9.5
	0, -2.0	), 0	0.7	9.0
	2.25, -2.0	0, 0	1.0	5.4
	3.0 , -2.0	0, 0	1.3	18.3
	3.5 , -2.0	), 0	1.6	11.0
	4.0 , -2.0	0, 0	1.9	13.8
x-z	-4.0 ,	, -0.1	7 27.4	11.9
	<b>-</b> 3.5 , 0	, -0.1	7 7.5	14.9
	-3.0 ,	, -0.1	7 3.4	13.2
	-2.25,	, -0.1	7 1.7	2.6
	0,	, -0.1	7 0.8	7.3
	2.25,	0, -0.1	7 1.7	1.9
	3.0 ,	, -0.1	7 3.5	11.0
	3.5 ,	, -0.1	7 7.5	13.4
	4.0,	, -0.1	7 27.4	18.7
	-4.0 ,	, -0.6	7 11.0	11.4
	<b>-</b> 3.5 , (	, -0.6	7 5.4	12.6

Plane	Poi: (x,y,z)		Theoretical Vmean, fpm	Experimental Vmean, fpm
x-z	-3.0 ,	0, -0.67	3.0	11.0
	<b>-</b> 2.25,	0, -0.67	1.5	1.7
	0,	0, -0.67	0.7	2.4
	2.25,	0, -0.67	1.5	1.9
	3.0 ,	0, -0.67	2.9	9.7
	3.5 ,	0, -0.67	5.4	10.5
	4.0 ,	0, -0.67	11.0	11.2
	-4.0 ,	0, -1.17	4.7	11.7
	<del>-</del> 3.5 ,	0, -1.17	3.2	12.9
	<b>-</b> 3.0 ,	0, -1.17	2.2	11.2
	<b>-</b> 2.25,	0, -1.17	1.3	2.0
	0,	0, -1.17	0.7	4.7
	2.25,	0, -1.17	1.3	2.4
	3.0 ,	0, -1.17	3.5	11.0
	3.5 ,	0, -1.17	7.5	13.4
	4.0 ,	0, -1.17	27.4	18.7
y-z	0, -	3.9, -0.17	0.55	18.4
	0, -	3.5, -0.17	0.58	10.6
	0, -	2.75,-0.17	0.63	14.9
•	0, -	2.0, -0.17	0.67	5.1
	0,	0, -0.17	0.75	6.2
	0,	2.0, -0.17	0.67	5.7

Plane	Point (x,y,z), ft.	Theoretical Vmean, fpm	Experimental Vmean, fpm
y-z	0, 2.75, -0.17	0.63	13.0
	0, 3.5, -0.17	0.58	10.5
	0, 3.9 , -0.17	0.56	13.6
	0,-3.9 , -0.67	0.54	13.5
	0,-3.5 , -0.67	0.56	16.2
	0,-2.75, -0.67	0.61	13.6
	0,-2.0 , -0.67	0.66	1.9
	0, 0, -0.67	0.73	2.4
	0, 2.0 , -0.67	0.66	2.14
	0, 2.75, -0.67	0.61	17.3
	0, 3.5 , -0.67	0.56	17.7
	0, 3.9 , -0.67	0.54	14.4
	0,-3.9 , -1.17	0.51	30.9
	0,-3.5 , -1.17	0.53	14.9
	0,-2.75, -1.17	0.58	19.1
	0,-2.0 , -1.17	0.62	1.9
	0, 0, -1.17	0.68	5.1
	0, 2.0 , -1.17	0.62	2.14
	0, 2.75, -1.17	0.58	13.2
	0, 3.5, -1.17	0.53	16.1
	0, 3.9 , -1.17	0.51	11.4

MICHIGAN STATE UNIVERSITY LIBRARIES

3 1293 03169 6887